

# Development and Validation of a Surrogate Mechanical Neck Prototype for Use in Helmet Certification Applications

M. K. Ogle<sup>1</sup>, J. P. Carey<sup>2</sup>, and C. R. Dennison<sup>1</sup>

<sup>1</sup> Biomedical Instrumentation Lab, Department of Mechanical Engineering, University of Alberta; <sup>2</sup> Department of Mechanical Engineering, University of Alberta

## ABSTRACT

*Critical to helmet certification methods is a neck model that offers lifelike head kinematics and neck kinetics in direct head impact testing. This study develops a phase 1 mechanical surrogate neck prototype that approximately matches the overall length of a 50<sup>th</sup> percentile human male. Our primary objective for the phase 1 neck was to test flexion/extension sagittal bending and dynamic head impact, for comparison to previous cadaveric literature, to ascertain whether the phase 1 neck can offer head kinematics and neck kinetics comparable to cadaveric models. Bending moments ranging up to 2 Nm and head impacts up to 5 m/s were simulated. When subjected to sagittal bending, the summation of all vertebral rotations was approximately 14 degrees for the phase 1 neck; less than the rotations of approximately 40 degrees presented in previous literature. In head impact, the phase 1 neck yielded kinematics within 40% of those reported in our selected cadaveric literature. Generally, the phase 1 neck yielded 22% less angular head acceleration and 77% lesser neck kinetics than those measured using HybridIII equipment in frontal, lateral, and rear head impacts. Head linear accelerations between the phase 1 and HybridIII were within 25%. Maximum inter-test variance of the phase 1 neck and HybridIII equipment were comparable (maximum 30% COV at peak magnitudes considering all data). The phase 1 neck sustained approximately 100 experiments without failure. Overall, we recommend re-design of the phase 1 neck toward allowing greater sagittal rotation, perhaps by approximating the neutral zone behavior noted in previous human cadaver literature. Additionally, we recommend further testing of cadaveric necks to yield a broader dataset to which we can compare, and further testing of the prototype neck to understand whether it yields head kinematics comparable to what has been measured for athletes.*

## INTRODUCTION

Individuals worldwide are at risk of suffering from traumatic brain injuries (TBIs), which can range from mild to severe. High-energy traumas such as motor-vehicle accidents, sport activities, or military operations can result in a TBI. These injuries to the brain are coupled with dire physical, behavioral, cognitive, and emotional effects, whose symptoms can interfere with normal brain function, and can significantly disrupt an individual's quality of life (Kay, 1993).

In Canada, an estimated \$26.8 billion was required to treat injuries in 2010 (Parachute, 2015). According to Stats Canada, sport related injuries account for over half of all injuries in youths and young adults and, among these, head injuries are consistently ranked in the top five (Billette, 2015).

Biomechanical research on TBI suggests a mechanical predictor variable for brain tissue damage is angular rotation of the head (Takhounts, 2013). This has opened a debate in standard organizations about the validity of current testing methods, and how testing could change to incorporate realistic approximations of the human. Central to this debate is the need of a fully developed head-neck model that offers realistic rotation of a surrogate head.

Multiple organizations have developed helmet certification standards to test the helmets ability to attenuate impact energy. The assumption, related to these methods, is attenuating impact energy transfer to a headform as an indicator the helmet can reduce head injury severity of a living human. Each standard offers a different assessment metric and head-neck component. The American hockey helmet standard includes a guided linear drop of a helmeted magnesium headform, fixed to a rigid metal rod, onto a horizontal anvil to measure peak linear acceleration (ASTM, 2016). The European motorcycle helmet standard tests a vertically dropped, neckless helmeted headform onto an angled anvil to assess the acceleration time history of the headform (UNECE, 2002). While this method allows for rotation in the headform, the fact the head is not tethered to a neck could raise questions related to the overall biofidelity of the method.

Other helmet assessment methods exist that use a headform mated to a neck model that allows for rotational head motion. For example, the NOCSAE football helmet standard certifies helmets using a pneumatic ram which impacts the helmeted headform on a 50<sup>th</sup> percentile HybridIII neck (NOCSAE, 2016). The standard is based on pass/fail criteria for severity index, rotational acceleration, and other measures (NOCSAE, 2016). Another example is the STAR rating system, which is not a certification but rather a proposed method to assess helmet performance and provide the public with performance data. The Hockey STAR uses as a performance metric formula that combines the probability of the head impact type in a single hockey season, and brain injury probability as a function of linear and angular acceleration (Rowson, 2015). The STAR experiment uses a 50<sup>th</sup> percentile HybridIII neck (Rowson, 2015). The HybridIII dummy was developed by the automotive industry to aid in evaluating the installed restraint systems in simulated vehicle collision scenarios (Mertz, 2015). While these standards specifically test for rotational acceleration of the headform, the HybridIII neck component is thought by many to be too mechanically stiff in bending to be considered a biofidelic neck model for helmet assessment.

The objective of this study is to develop what we term a phase 1 mechanical surrogate neck prototype. Our phase 1 efforts focus on establishing whether our neck model is repeatable and can survive multiple tests without failure. Additionally, our phase 1 experiments comprise quasi-static bending in the sagittal plane as well as dynamic testing at several impact speeds, and comparing the results to available cadaveric data from several literature sources.

## METHODS

Many published literature on cadaver head kinematics and neck kinetics focus on the analysis of 50<sup>th</sup> percentile male human. Therefore, the overall length of the phase 1 prototype approximately matched that of a 50<sup>th</sup> percentile human male (Vasavada, 2008). The overall neck, vertebral body, and intervertebral disc dimensions of the neck can be found in Table 1.

Table 1: Dimensions of the phase 1 mechanical surrogate neck prototype

Phase 1 Prototype Neck Dimensions		
Overall Neck Dimensions		
Measurement Direction	Measurement (mm)	
Overall Length	115.58	
Neck Circumference (max.)	633.41	
Vertebral Bodies and Intervertebral Discs	Measurement (mm)	
	Width	Depth
C1 Vertebral Body and C1-2 Disc	16.91	15.45
C2 Vertebral Body and C2-3 Disc	16.91	15.45
C3 Vertebral Body and C3-4 Disc	16.51	15.25
C4 Vertebral Body and C4-5 Disc	17.00	15.50
C5 Vertebral Body and C5-6 Disc	18.5	16.50
C6 Vertebral Body and C6-7 Disc	20.5	17.50
C7 Vertebral Body and C6-7 Disc	22.5	17.50

A detailed computer model of the phase 1 neck can be found in **Error! Reference source not found..** The vertebral bodies were manufactured from waterjet cut aluminum (6061-T6). The neck contained three tensioned steel cables, one that passed through the center of each vertebral body, and one through each posterior element. The intervertebral discs were 3D printed rubber (TangoPlus – FullCure 930, 3D Printers Canada, Vaughan, ON). The superior and inferior ends of the discs were angled to achieve lordosis (Vasavada, 2008). The neck assembly was encased in silicone, to simulate the viscera (Ecoflex 00-30, Smooth-On Inc., Macungie, PA) (Sparks, 2015). Including the nodding joint, the entire phase 1 neck had a mass of 1.01 kg.

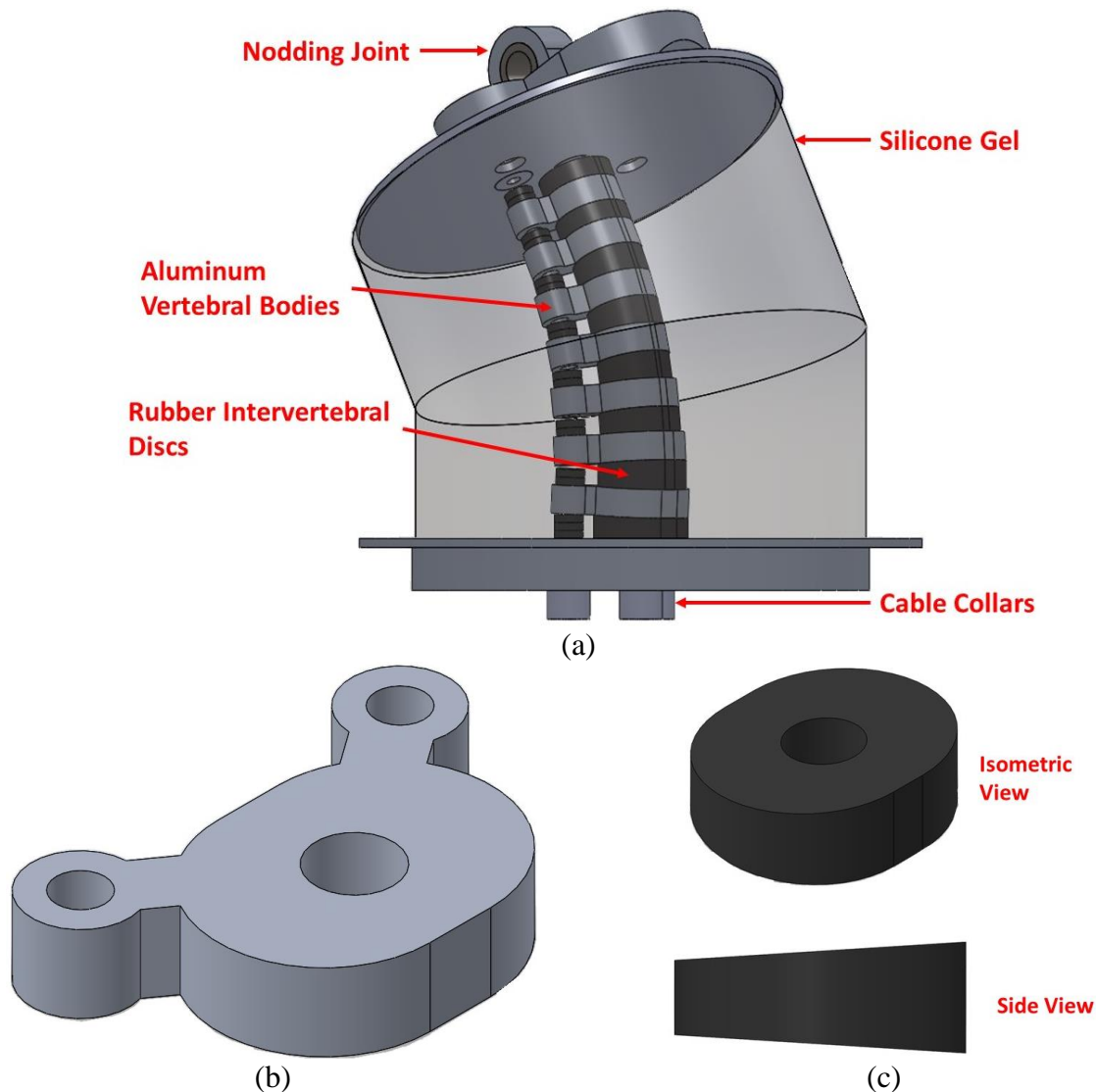


Figure 1: Phase 1 mechanical surrogate neck prototype components, (a) entire phase 1 neck assembly, (b) sample vertebral body structure, and (c) sample intervertebral disc structure. Note the nodding joint allows the neck to attach to a HybridIII head.

### Quasi-static sagittal flexion-extension

Quasi-static testing included a six-degree of freedom robotic platform (Model R2000 Rotopad, Mikrolar Inc., Hampton, NH). While one end of the neck was held stationary, the opposing end was fastened to a six-axis load cell (MC3A Force/Torque Sensor, AMTI Inc., Watertown, MA) (**Error! Reference source not found.**). Metal rods were threaded into the aluminum vertebral bodies and extended out of the silicone. Markers adhered to the rods allowed for translation to be video recorded for post-hoc vertebral body angular motion analysis (SONY HDR-XR160 Camcorder, Sony Electronics Inc., San Diego, CA).

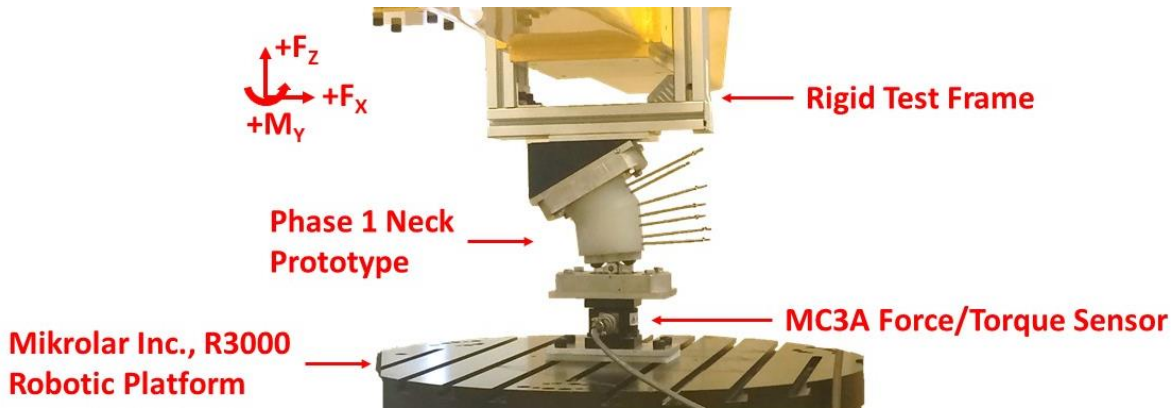


Figure 2: Annotated image of phase 1 mechanical surrogate neck prototype mounted onto Mikrolar 6 degrees of freedom robotic platform

Table 2 contains the quasi-static test matrix. The range of applied moments in the sagittal plane included  $\pm 1.5$  Nm and  $\pm 2.0$  Nm, encompassing moments within the flexion/extension elastic range of a human cervical spine specified in previous work (Camacho, 1997, Nightingale, 2006, and Wheeldon, 2006). The test protocol was moment controlled, and center of rotation was positioned at the mid-height of the phase 1 neck. The load cell recorded forces and moments in the x-, y-, and z-directions. While efforts were made to apply pure moments, limitations related to travel of the robot platform led to forces in the y-direction, moments about the x-axis, and moments about the z-axis at values up to 2.59 N, 0.59 Nm, and 0.07 Nm, respectively. Future refinements to our protocol will attempt to minimize these undesired loads/moments.

Table 2: Distribution of quasi-static tests in sagittal plane of phase 1 mechanical surrogate neck prototype

Number of Quasi-Static Tests			
Stationary End	Applied Moment (Nm)		Total
	$\pm 1.5$	$\pm 2.0$	
Inferior	3	3	6
Superior	3	3	6
All	6	6	12

Prior to each test, the robotic platform was positioned such that 0 Nm were experienced in the x-, y-, and z-directions. The robotic platform rotated at 0.1 to 0.3 deg/sec until the maximum moments were achieved. A single test included three repeated flexion to extension cycles of the phase 1 neck. The applied moment was collected and saved at 20 Hz (LabVIEW v8.5, National Instruments, Austin, TX). Kinovea motion tracking software was used to track the translational marker displacement of the rods (Kinovea v.0.8.15). The resulting translational displacements were input to MATLAB software, where digital filtering techniques and inter-vertebral angular displacement calculations were applied (MATLAB R2016b, MathWorks, Natick, MA). The sum of inter-vertebral angular displacements from C1-7 were then plotted against applied moment, and compared to literature.

It is important to note our simple, two-dimensional planar method for determining rotation in the sagittal plane differs from more accurate stereoscopic methods presented in previous

literature. Our phase 1 objective was to assess the overall bending compliance. Following phase 1 efforts, we will employ stereoscopic methods and co-ordinate transform methods to determine the relative magnitudes of rotation at each vertebral level.

### Dynamic impact in guided free-fall

The experimental setup for dynamic testing included a guided linear drop of an un-helmeted HybridIII ATD headform, fixed to the phase 1 neck, onto a modular elastomer programmer (MEP) (Figure 3). This impact surface allowed for unhelmeted impacts while ensuring the test equipment was not damaged. Details of the drop tower experiment can be found in Knowles et al. (Knowles, 2017). Due to the compliancy of the phase 1 neck, the HybridIII headform was fixed into the correct position using breakaway cables. The dynamic tests were recorded with dual high-speed video cameras for post-hoc observation of impacts (Phantom v611, Vision Research Inc., Wayne, NJ).

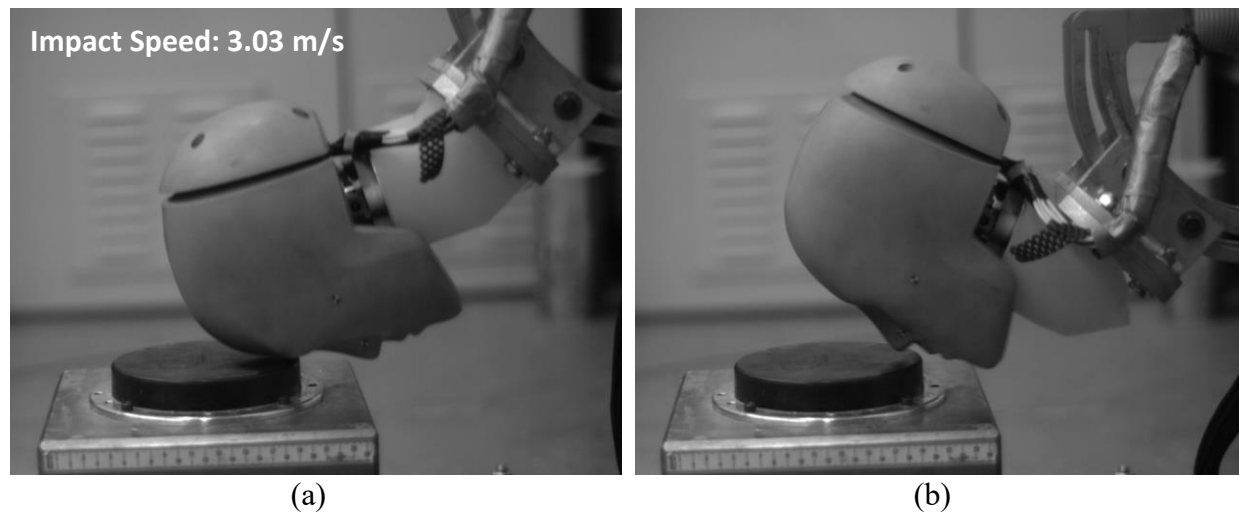


Figure 3: High speed image of HybridIII headform and phase 1 mechanical surrogate neck prototype, (a) just prior to 3.0 m/s frontal impact, (b) just after 3.0 m/s frontal impact

Table 3 details the HybridIII neck to phase 1 neck comparison matrix. The impact velocity was chosen to be 1.5 m/s, and impact locations included front, rear, side, and crown of the HybridIII ATD headform. The HybridIII headform COG kinematics and upper neck kinetics between the HybridIII neck and phase 1 neck were compared. It was assumed the kinematic and kinetic differences observed at the minimum impact speed of the cadaveric comparison (described below) would be similarly, or more drastically, scaled at higher impact speeds.

Table 3: Distribution of 1.5 m/s dynamic impact comparison of HybridIII ATD headform fixed to HybridIII neck and phase 1 mechanical surrogate neck prototype, categorized by HybridIII ATD headform impact location

Number of Dynamic Tests at 1.5 m/s Impact Speed			
Impact Location	HybridIII Neck	Phase 1 Neck	Total
Forehead	3	3	6
Rear	3	3	6
Side	3	3	6
Crown	3	3	6
All	12	12	24

Table 4 details the human cadaver to phase 1 neck comparison matrix. Impact velocities ranged from 1.5-5.0 m/s, and impact locations included forehead, rear, and side of the HybridIII headform. The head kinematics and upper neck kinetics between the human cadaver and phase 1 neck were compared. These test conditions were gleaned from previous studies on injury and impact response corridors of human cadaver cervical spine segments (Advani, n.d., Rizzetti, 1997, and Yoganandan, 2011).

Table 4: Distribution of dynamic impact tests of HybridIII ATD headform fixed to phase 1 mechanical surrogate neck prototype, categorized by impact speed and HybridIII headform impact location

Number of Dynamic Tests									
Impact Location	Impact Speed (m/s)								Total
	1.5	2.0	2.5	3.0	3.5	4.0	4.5	5.0	
Forehead	3	3	3	3	3	3	3	3	24
Rear	3	3	3	3	3	3	3	3	24
Side	3	3	3	3	3	3	3	3	24
All	9	9	9	9	9	9	9	9	72

It is important to note the impact experimental method used in the present work (guided free-fall) differs from that in literature to which we compare. The phase 1 objective was to observe the differences in head kinematics and upper neck kinetics in direct head impacts. As the phase 1 neck is further developed to better match the compliancy of a human neck, we will employ impact methods to the headform that allow more direct comparison to previous literature.

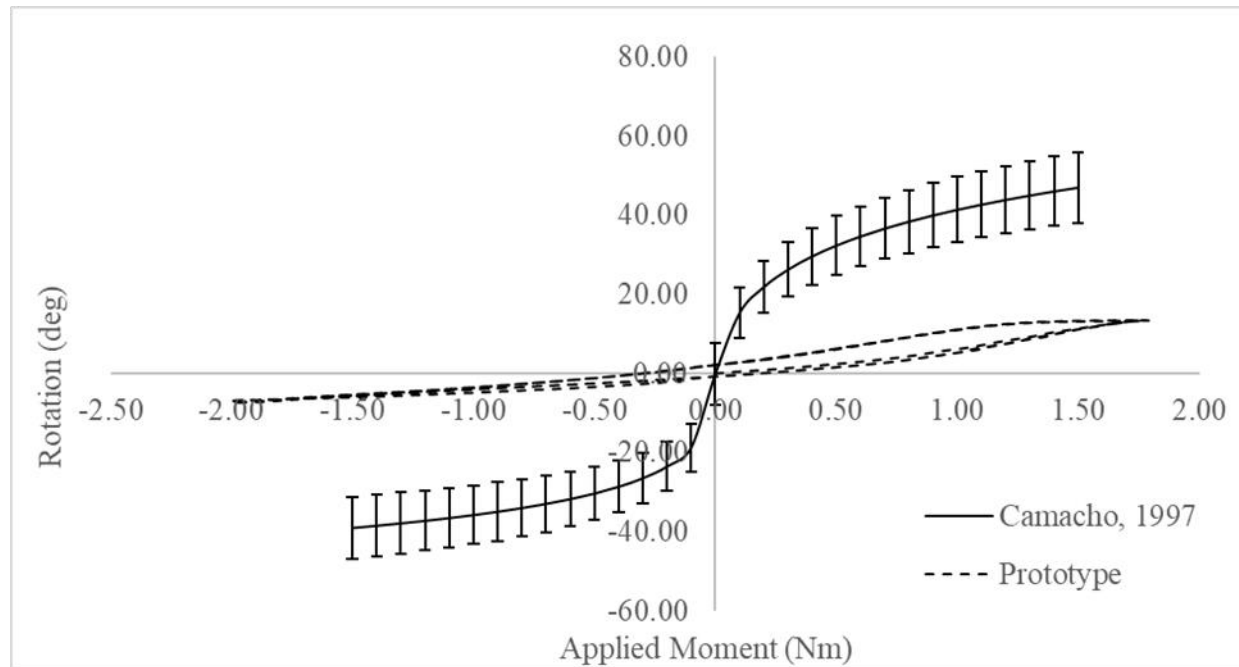
The HybridIII headform was instrumented with nine uniaxial accelerometers arranged in a 3-2-2 array (model 64C-2000-360, Measurement Specialties Inc., Hampton, VA). From these accelerometers, the resultant linear acceleration was measured. The resultant angular accelerations about the center of mass were calculated using methods presented by Padgaonkar et al (Padgaonkar, 1975). The upper neck forces and moments were measured using a six-axis upper neck load cell (model N6ALB11A, mg sensor GmbH, Iffezheim, Germany). Impact speeds were measured using a purpose-built velocity gate. The coordinate system prescribed in SAE standard method J211 was used for the HybridIII headform (SAE, 2003).

The impact linear acceleration and upper neck kinetics were collected and saved at 100 kHz using National Instruments software (PXI 6251 and LabVIEW v8.5, Austin TX). The analog voltages were filtered from the hardware with a cut-off frequency of 4 kHz prior to post-hoc software filtering to the appropriate Channel Frequency Classes detailed in SAE J211 (SAE, 2003).

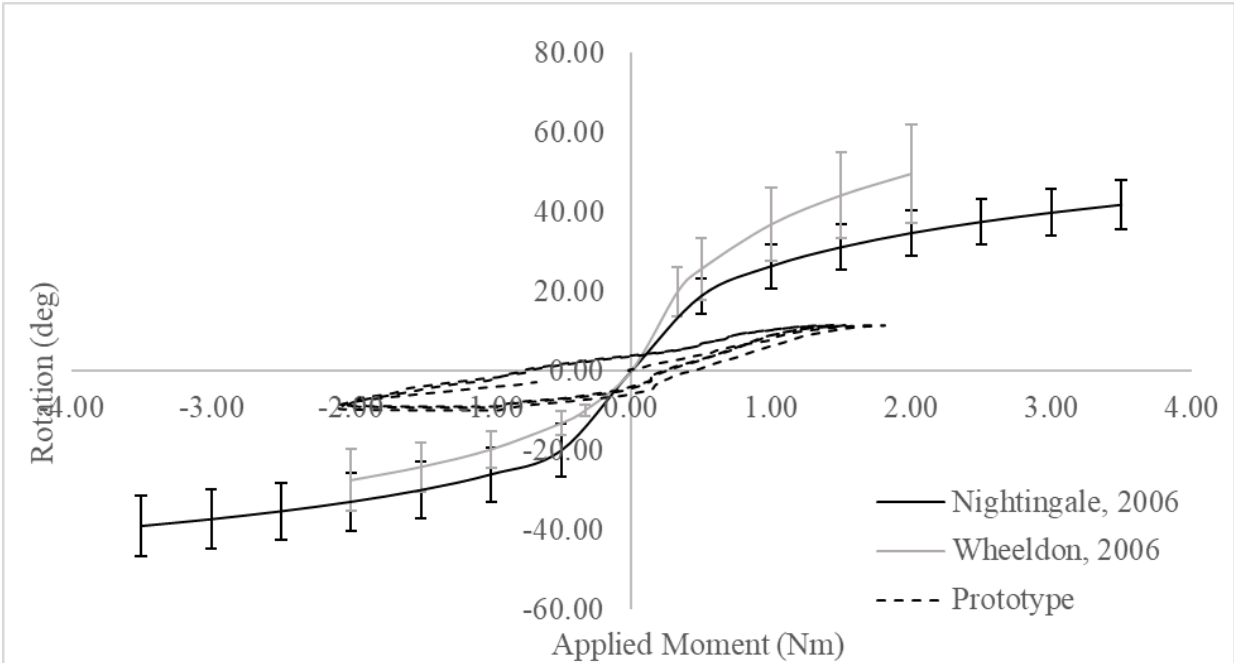
## RESULTS

### Quasi-static sagittal flexion-extension results

Figure 4 presents sample inferiorly and superiorly loaded quasi-static flexibility comparisons of the phase 1 neck at an applied moment of  $\pm 2.0$  Nm to averaged cadaver data presented in literature (Camacho, 1997, Nightingale, 2006, and Wheeldon, 2006). A sample, rather than an average, of the data set was chosen to convey how the phase 1 neck rotates over three flexion-extension cycles. Over the 12 trials, the maximum difference in peak flexion angle and peak extension angle between the phase 1 neck to data published by Camacho is 83.8% and 78.6%, data published by Nightingale is 84.7% and 86.8%, and data published by Wheeldon is 77.0% and 82.7%, respectively.



(a)



(b)

Figure 4: Summated angular displacement from C1-7: (a) superior end of phase 1 mechanical surrogate neck prototype stationary, (b) inferior end of phase 1 mechanical surrogate neck prototype stationary. Note: the data published by Camacho et al. hold the superior end of the cadaver neck stationary, data published by Nightingale et al. and Wheeldon et al. hold the inferior end of the cadaver neck stationary.

Figure 5 presents sample average and standard deviation of the phase 1 neck rotations at applied moments ranging  $\pm 2.0$  Nm. Table 5 summarizes the inter-test variability. Over the 12 trials, the maximum summation of the angular displacement in flexion is 13.47 degrees, maximum extension is -8.84 degrees, and maximum standard deviation is 4.85 degrees. The maximum inter-test difference in angular displacement summated from C1-7 in flexion/extension is 14.3% and 26.0%, respectively.

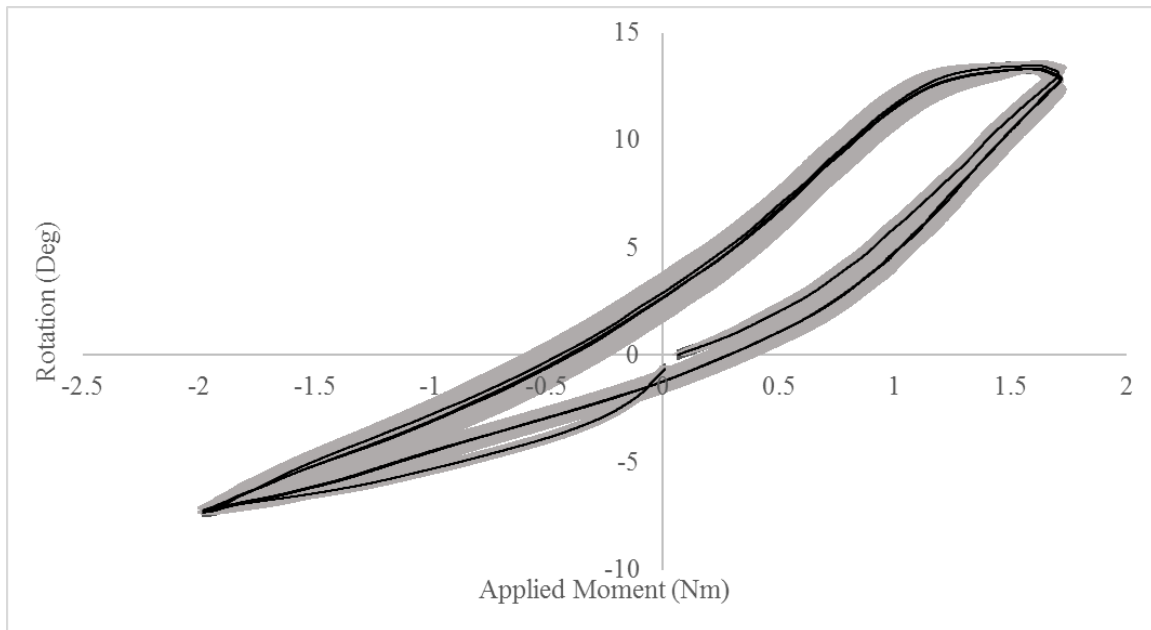


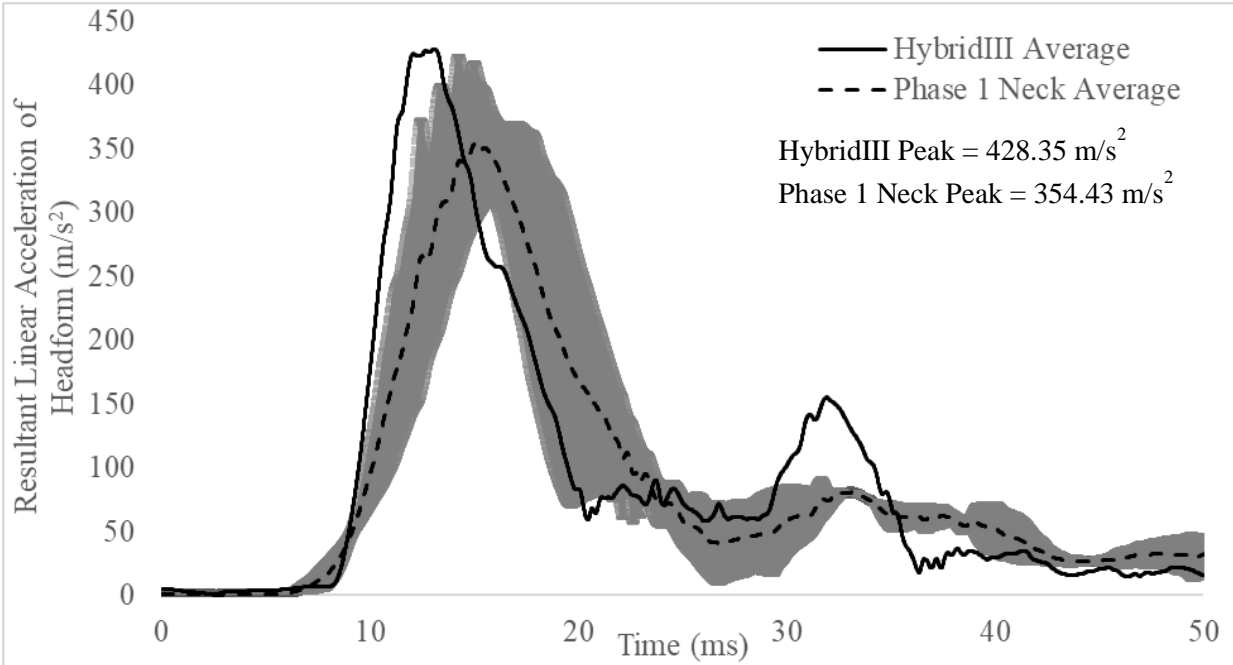
Figure 5: Sample averaged summation of angular displacement of inferiorly loaded phase 1 mechanical surrogate neck prototype from C1-C7 versus  $\pm 2.0$  Nm moment. Greyed areas are  $\pm 1$  SD of three averaged tests (solid).

Table 5: Summary of inter-test variability of quasi-static sagittal flexion and extension tests of the phase 1 mechanical surrogate neck prototype

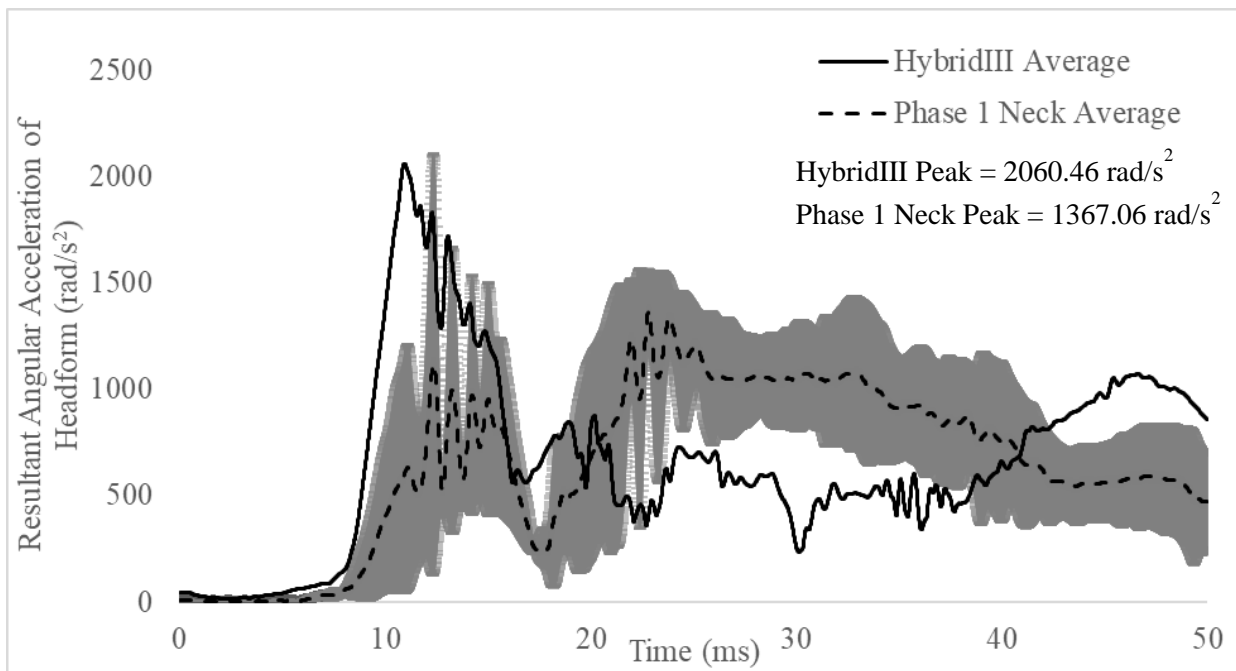
Average Peak Values and Maximum Standard Deviation of Quasi-Static Tests			
Test Name	Average Flexion Peak	Average Extension Peak	SD
Base_1.5	9.95	-5.77	4.69
Base_2.0	13.47	-7.33	1.02
Top_1.5	7.64	-5.76	2.20
Top_2.0	11.00	-8.84	4.85

### Dynamic impact in guided free-fall kinematic and kinetic results

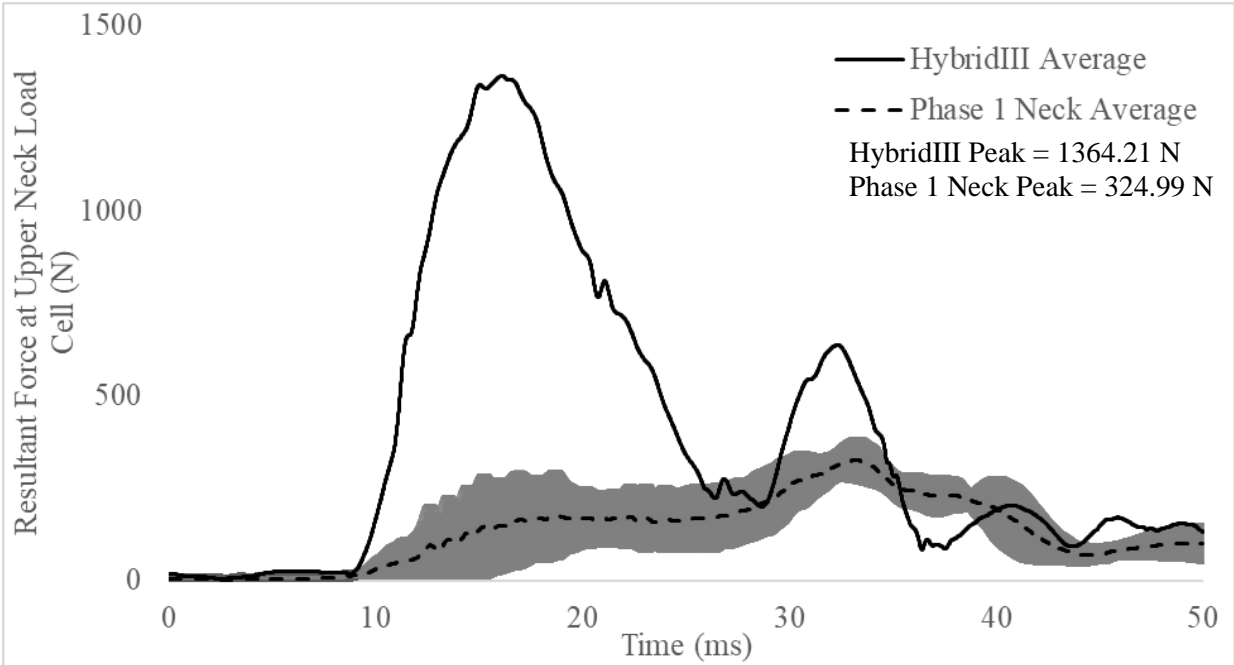
Figure 6 compares the average resultant head kinematics and upper neck kinetics at 1.5 m/s frontal impact between the phase 1 neck and the HybridIII neck. As shown, peak linear accelerations averaged within 17.3% and angular accelerations within 33.7%, while the phase 1 neck had 76.2% lower forces and 52.2% lower moments than the HybridIII neck. To summarize, focusing on angular acceleration, the phase 1 neck yielded peak angular accelerations that were 34%, 28%, and 11% less than those found for the HybridIII for frontal, lateral, and rear impacts, respectively. For crown impacts, phase 1 neck angular accelerations were 31% greater. For all impact locations, linear accelerations between the phase 1 neck and Hybrid were within 25% of one another.



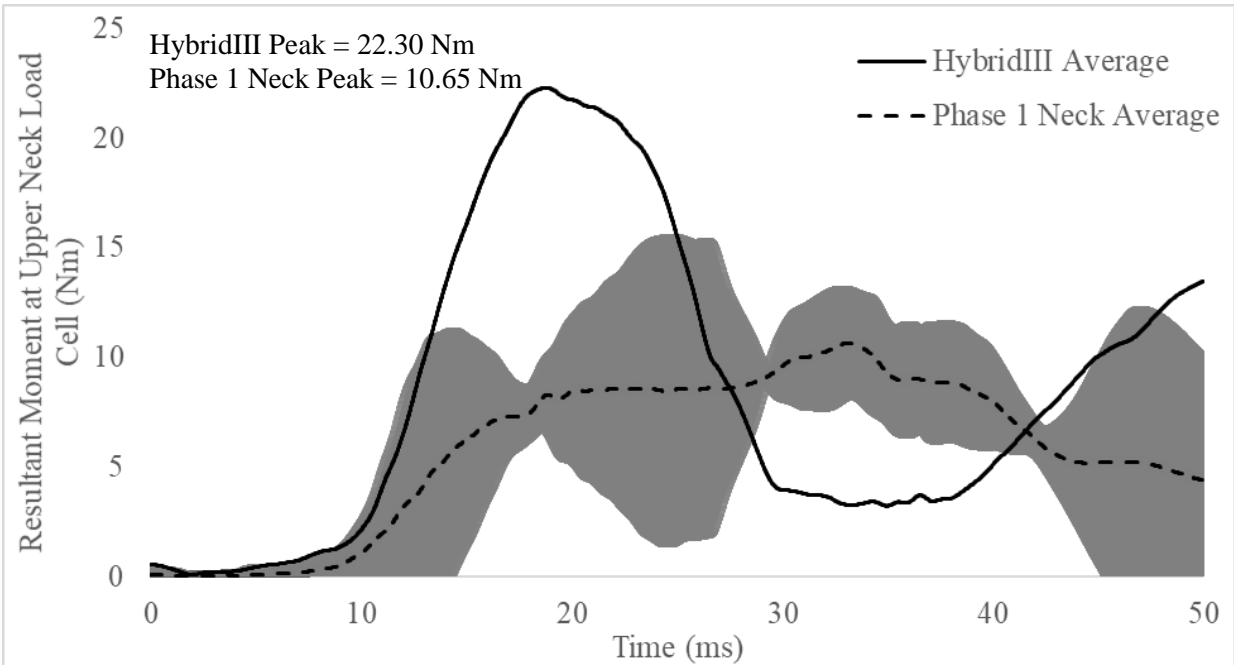
(a)



(b)



(c)



(d)

Figure 6: Averaged dynamic comparison of HybridIII ATD neck model and phase 1 mechanical surrogate neck prototype at 1.5 m/s frontal impact, (a) resultant COG linear acceleration of headform, (b) resultant COG angular acceleration of headform, (c) resultant upper neck forces, (d) resultant upper neck moments. Greyed areas show  $\pm 1$  SD of three averaged phase 1 neck tests.

Figure 7 compares the x-component linear acceleration of a 3.0 m/s frontal impact between the phase 1 neck to data presented by Advani et al. (Advani, n.d.). The cadaver data includes dynamic head COG linear acceleration calculated by differentiation from high speed videos (Advani, n.d.). The percent difference in peak values between the phase 1 neck and cadaver data is 25.8%.

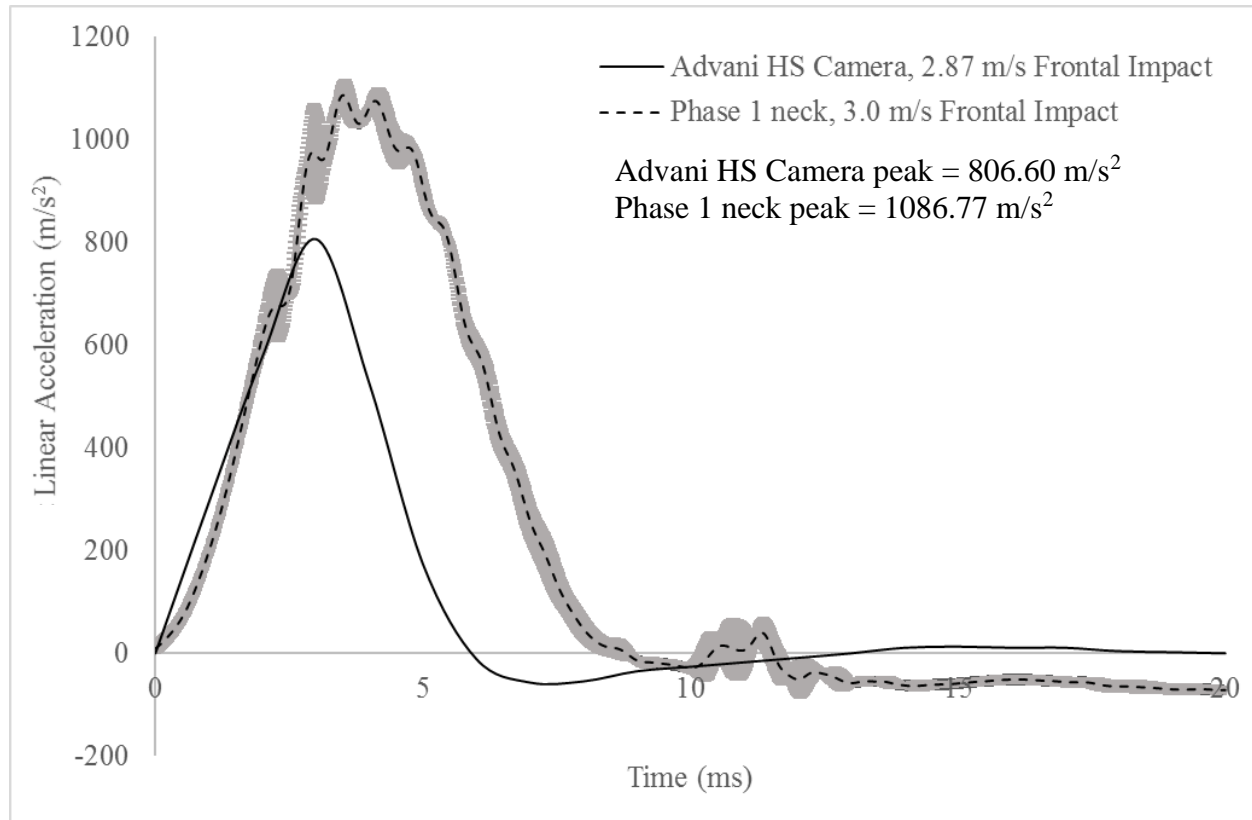


Figure 7: Comparison of x-component linear accelerations of headform COG at 3.0 m/s frontal impact between phase 1 mechanical surrogate neck and adapted data presented by Advani et al. (Advani, n.d.). Greyed areas show  $\pm 1$  SD of three averaged phase 1 neck tests.

Figure 8 and Figure 9 present the comparison of resultant linear acceleration and angular acceleration about the y-axis of head COG between averaged phase 1 neck 5.0 m/s rear impacts to occipital impact data presented by Rizzetti et al., respectively (Rizzetti, 1997). The percent difference in peak resultant linear acceleration between the phase 1 and cadaver data is 45.5%, and in rotational acceleration about the y-axis is 36.7%. The comparison of rigid impacts between the phase 1 neck model and cadaver data is summarized in Table 6.

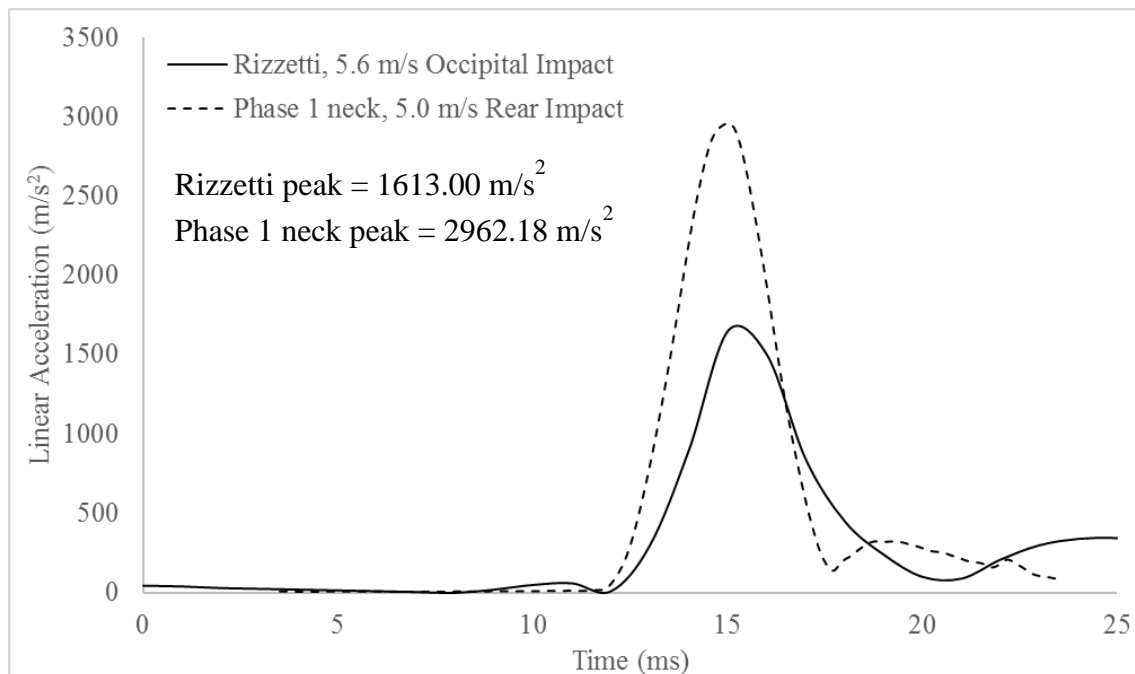


Figure 8: Comparison of resultant linear acceleration of COG between averaged of three 5.0 m/s HybridIII head rear cap impacts fixed to phase 1 mechanical surrogate neck prototype and an adapted 5.6 m/s occipital impact presented by Rizzetti et al. (Rizzetti, 1997).

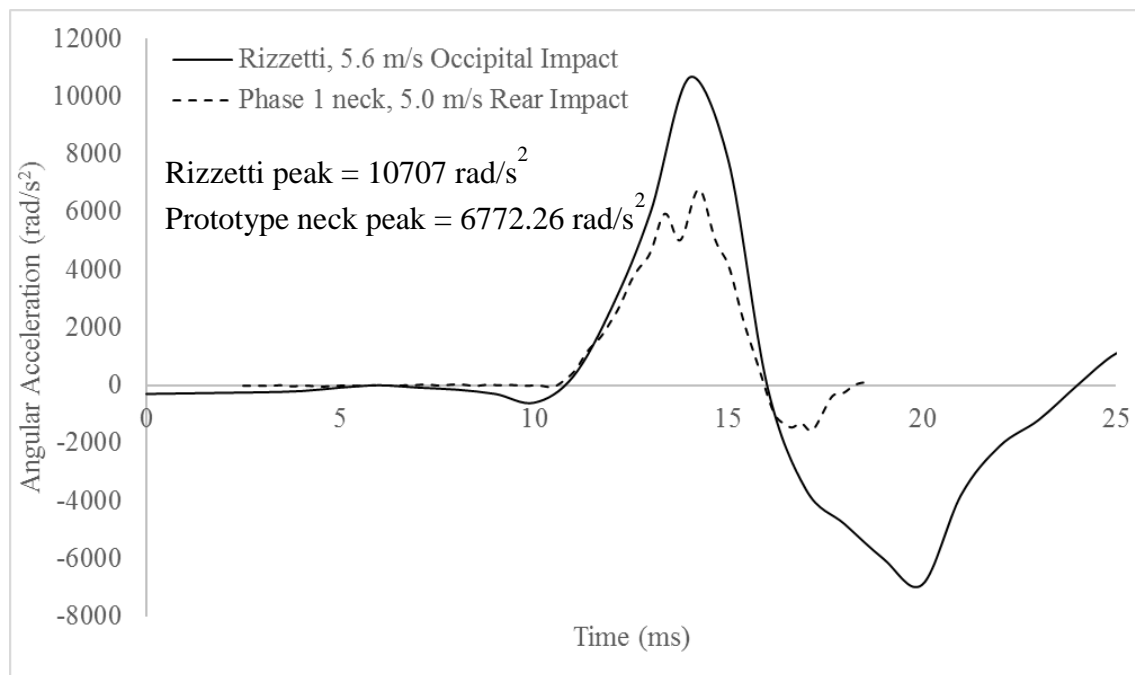


Figure 9: Comparison of rotational acceleration about the y-axis between between averaged of three 5.0 m/s HybridIII head rear cap impacts fixed to phase 1 mechanical surrogate neck prototype and an adapted 5.6 m/s occipital impact presented by Rizzetti et al. (Rizzetti, 1997).

Table 6: Summary of percent difference in peak head kinematic values between phase 1 mechanical neck prototype and rigid impact data presented by Rizzetti et al. at an impact speed of approximately 5.0 m/s (Rizzetti, 1997)

Head COG Kinematic Values						
Configuration	Rizzetti et al. Rigid Impact		Phase 1 Neck		Comparison	
	Linear Accel. (m/s <sup>2</sup> )	Rot. Accel. (rad/s <sup>2</sup> )	Linear Accel. (m/s <sup>2</sup> )	Rot. Accel. (rad/s <sup>2</sup> )	% Difference Linear Accel.	% Difference Angular Accel.
Frontal	1373	-	2315.37	5915.71	40.70	-
Occipital	1613	10707	2962.18	6772.26	45.54	36.75

Figure 10 and Figure 11 present the comparison of resultant forces and moments at the occipital condyles of a lateral impacts between the phase 1 neck at 5.0 m/s and data presented by Yoganandan et al. at 7.0 m/s, respectively (Yoganandan, 2011). The percent difference in peak upper neck forces between the phase 1 and cadaver data of is 31.6%, and upper neck moments is 73.1%. The time window of the phase 1 data has been shortened to reflect the initial impact of the HybridIII headform.

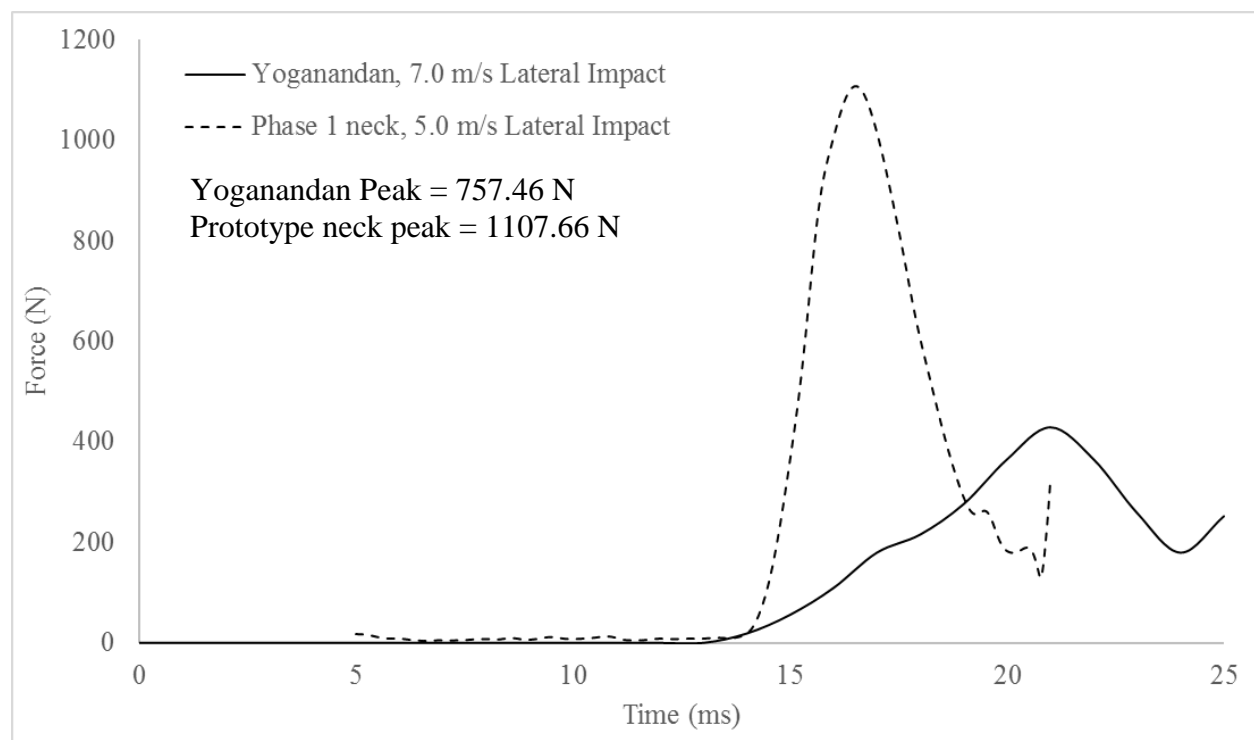


Figure 10: Comparison of resultant upper neck forces at occipital condyles between average of three phase 1 mechanical surrogate neck prototype neck 5.0 m/s lateral impacts and adapted lateral impact data presented by Yoganandan et al. at 7.0 m/s (Yoganandan, 2011)

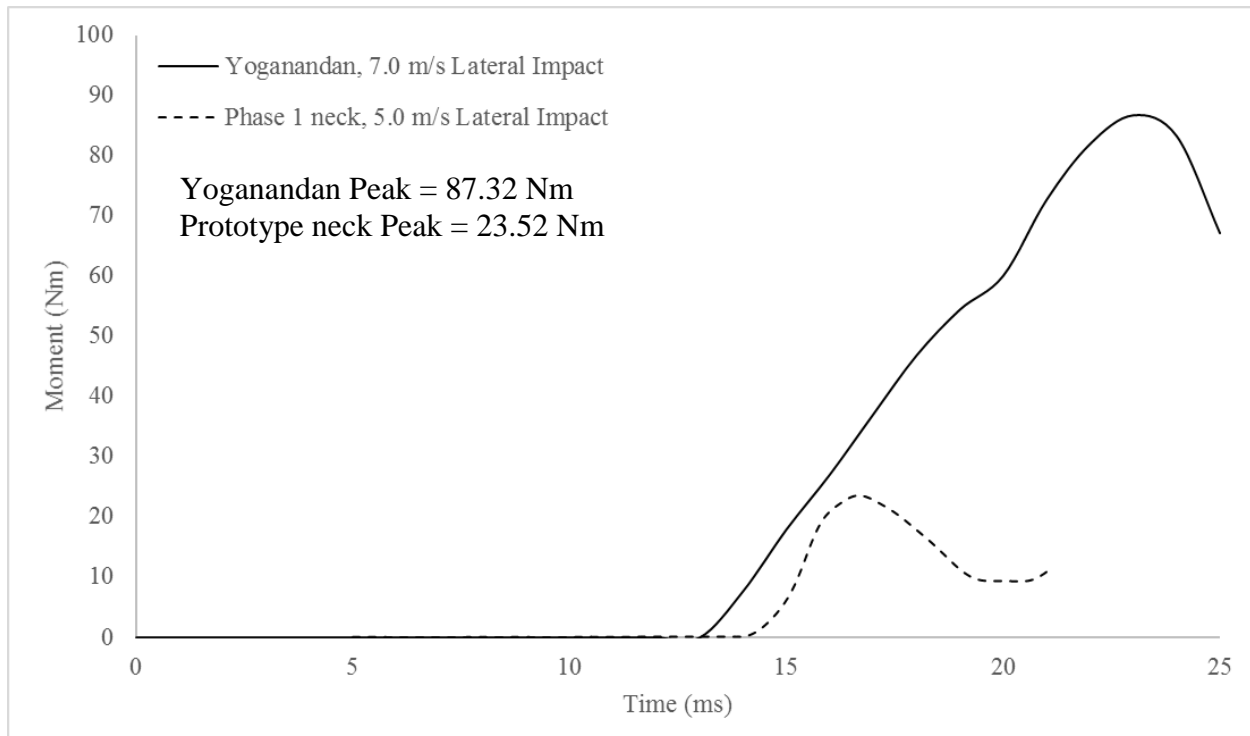
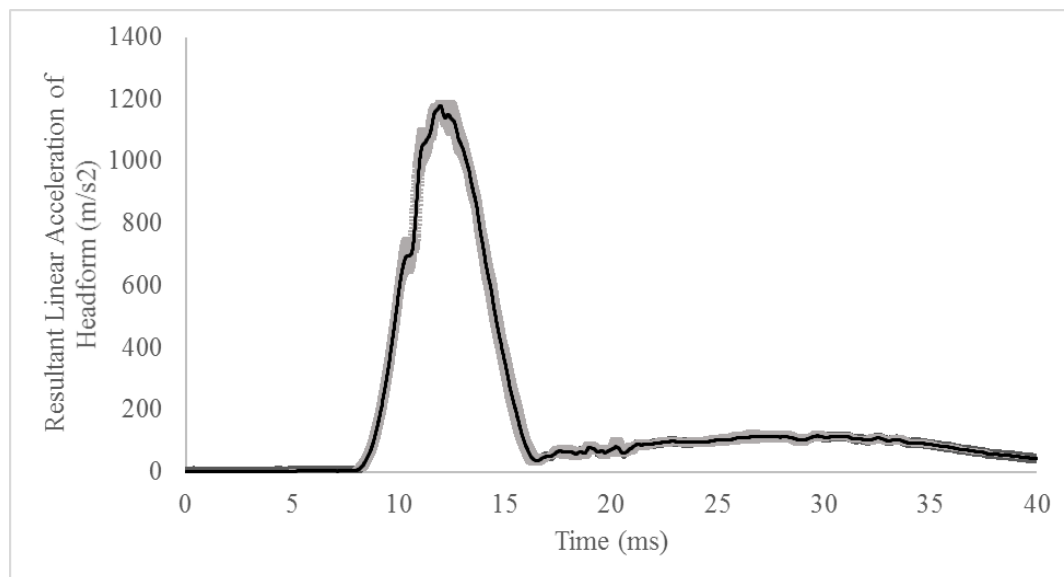
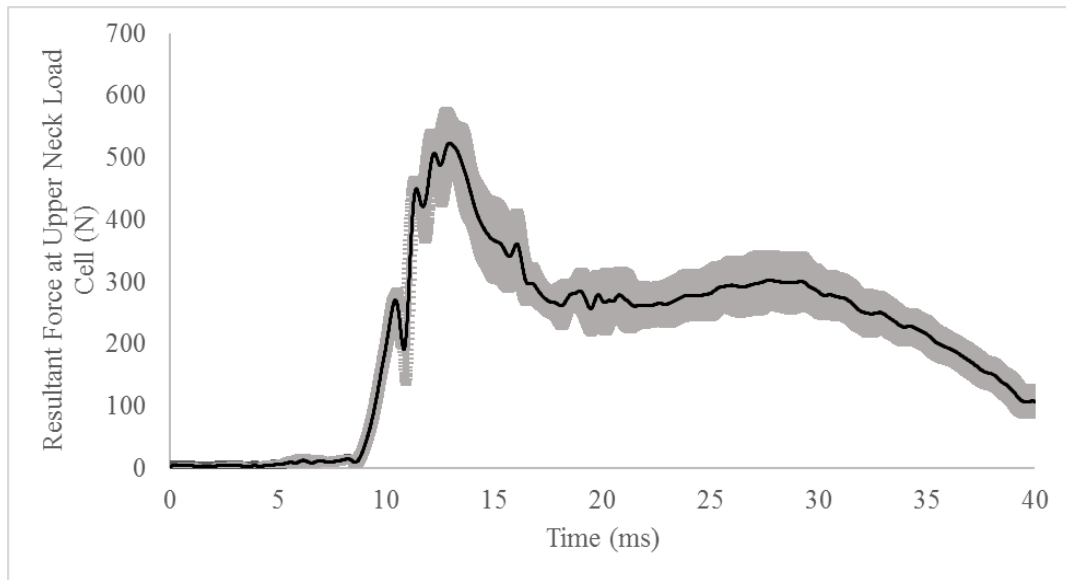


Figure 11: Comparison of resultant upper neck moments at occipital condyles between between average of three phase 1 mechanical surrogate neck prototype neck 5.0 m/s lateral impacts and adapted lateral impact data presented by Yoganandan et al. at 7.0 m/s (Yoganandan, 2011)

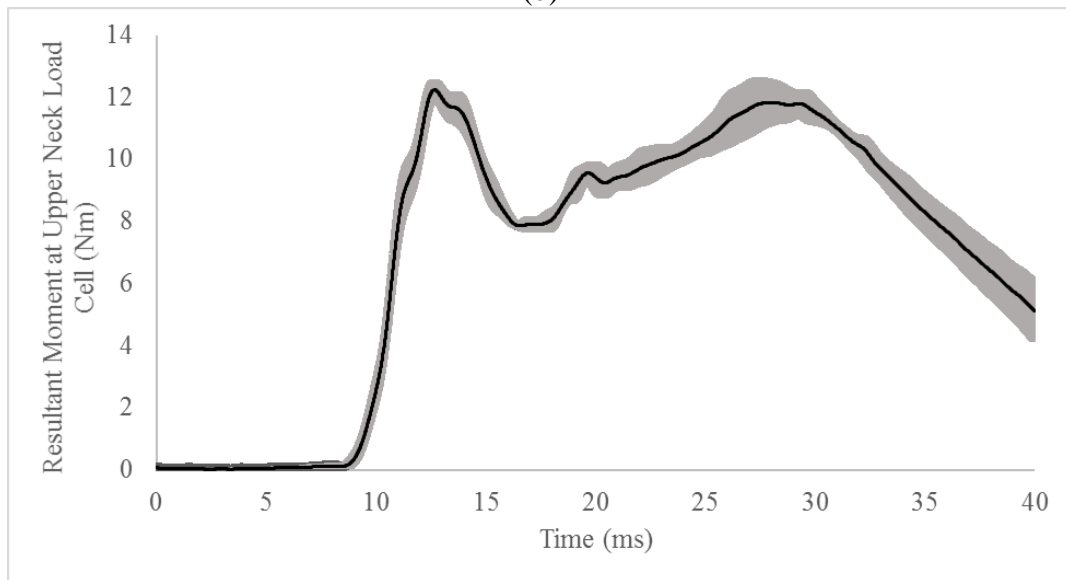
Figure 12 presents sample dynamic variability of the head kinematics and upper neck kinetics of a 3.0 m/s frontal impact of the phase 1 neck. Over the 72 trials, the maximum inter-test difference in peak resultant linear acceleration of the headform COG is 25.6%, peak upper neck force is 35.6%, and peak upper neck moment is 28.9%.



(a)



(b)

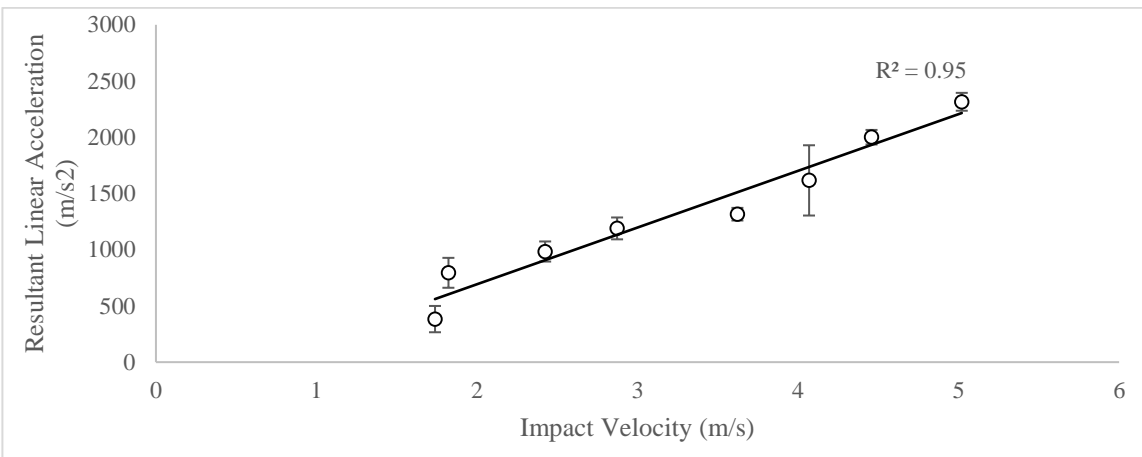


(c)

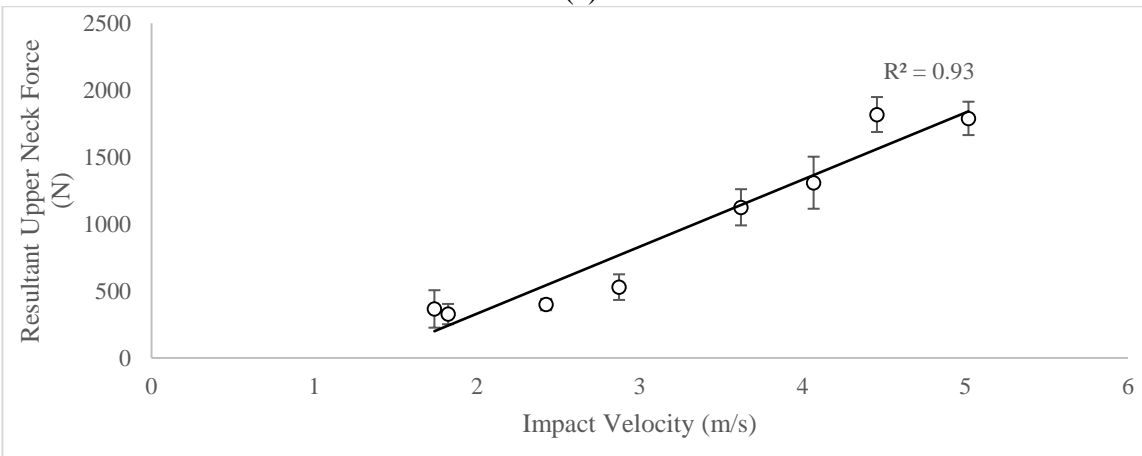
Figure 12: Sample resultant head kinetics and upper neck kinematics of HybridIII ATD headform fixed to phase 1 mechanical surrogate neck prototype of 3.0 m/s frontal impact, (a) head COG linear acceleration, (b) upper neck forces, (c) upper neck moments. Greyed areas show  $\pm 1$  SD of three averaged phase 1 neck tests.

### Simple Linear Regressions

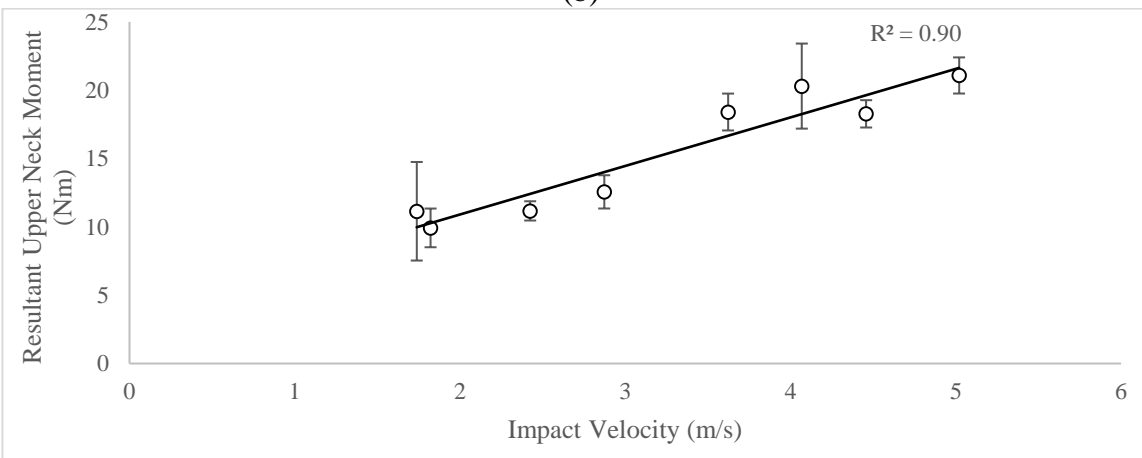
Figure 13 presents a sample simple linear regression model of the resultant linear acceleration of the headform COG, upper neck forces, and upper neck moments for the dynamically loaded phase 1 neck with  $R^2$  values displayed. These results convey the peak measures scale approximately linearly with impact speed as evidenced by  $R^2$  more than 0.90 for the presented data.



(a)



(b)



(c)

Figure 13: Sample simple linear regression models for dynamic frontal loading of the phase 1 mechanical surrogate neck prototype with  $R^2$  value displayed, (a) resultant linear acceleration of headform COG, (b) resultant upper neck forces, (c) resultant upper neck moments.

## DISCUSSION

This paper presents our phase 1 efforts to develop a mechanical surrogate neck prototype. Our phase 1 experimental efforts focused on comparing rotational stiffness in flexion-extension to available literature, and comparing head kinematics and neck kinetics in impact testing the phase 1 neck to both the 50<sup>th</sup> percentile HybridIII neck and to human cadaver literature.

The quasi-static setup of the phase 1 neck differed from literature such that the rotating end of the neck occurred at the same point where the moments were measured. The data published by Camacho et al. included superior fixation of the inverted halo-T2 spine segment to a load cell, and an eccentric force couple loaded the inferior end to observe the individual inter-vertebral angular displacements (Camacho, 1997). Nightingale et al. sectioned cervical spine segments from O-C3, C4-C5, and C6-C7 to observe flexural stiffness differences in the upper, middle, and lower cervical spine (Nightingale, 2006). The inferior end of the spinal segments were rigidly fixed to a load cell, and pneumatic pistons loaded the superior end of the spinal segments to generate a force-couple (Nightingale, 2002). Wheeldon et al. observed the individual angular displacements of C2-T1 spinal columns by applying pure moments to the superior end while rigidly fixing the inferior end to a load cell (Wheeldon, 2006). In all published results, the musculature of the neck segments were removed. To compare the overall flexion/extension range of motion from the phase 1 neck to the data presented in the chosen literature, the angular displacements and variances were summed and contrasted to the phase 1 neck results.

The summation of vertebral rotations from the phase 1 neck is lesser, by approximately 80%, than those reported from previous authors (Camacho, 1997, Nightingale, 2006, and Wheeldon, 2006). As stated in the Methods, our goal in phase 1 is to ascertain the overall rotational stiffness in quasi-static bending. Additionally, we reiterate the center of rotation used in our video analysis differs from that used by previous authors. Nevertheless, our data indicates the phase 1 neck offers greater stiffness than what is expected from the cadaver. We speculate that one contributor to this is the fact the phase 1 neck has no neutral zone, where vertebral rotations occur without significant applied moments (Figure 4a, between 0 Nm and 0.25 Nm), a phenomena that has been observed for the osteoligamentous cervical spine (Crawford, 1998). We speculate phase 1 neck re-design may be necessary to approximate such neutral zone behavior. Following this re-design, we plan to employ stereo photogrammetry to ascertain vertebral motions in a manner that more closely matches previous efforts (Camacho, 1997, Nightingale, 2006, and Wheeldon, 2006).

Our comparisons between the HybridIII head-neck and HybridIII head mated to the phase 1 neck indicate linear accelerations were on average within 17% and angular accelerations were within 34%, but neck kinetics for the phase 1 neck were 76% (resultant forces) to 52% (resultant moments) less (Figure 6).

When comparing phase 1 neck results to cadaveric literature in impact testing, linear accelerations were within approximately 40% of one another and rotational accelerations were within approximately 30%. While these results could be argued as promising, we acknowledge the amount of cadaver data to which we compare is limited and there were important differences between our drop impact experiments and the experiments to which we compare. The data published by Advani et al. were results from pendulum impacts (Advani, n.d.). Rizzetti et al.

published data from pneumatic piston impacts (Rizzetti, 1997). Yoganandan et al. tested cadaver subjects using an electrohydraulic device which pulled a cable to rotate the head (Yoganandan, 2011). We acknowledge our ongoing efforts will need to assess these head loading paradigms and we will need to undertake cadaveric testing with post-mortem subjects to allow direct comparison to a greater number of the test cases than detailed in Table 4.

Another limitation in the presented work is that we do not have a dataset from living humans to which we can compare. To our knowledge, it is an open question whether or not the neck of a post-mortem subject is a realistic model for the living human. We acknowledge that our mechanical surrogate, even if refined to match behavior of a cadaveric neck, might not match the mechanics of a living human. A possible solution could be to attempt to match head kinematics measured on living athletes in a laboratory setting where sport impacts can be recreated.

## CONCLUSIONS

The purpose of this study was to develop and compare the quasi-static and dynamic experimental results of a phase 1 mechanical surrogate neck prototype to the human cadaver. The quasi-static testing applied moments in the sagittal plane. The dynamic testing included frontal, lateral, and occipital impacts to the headform at several speeds. Phase 1 results suggest the phase 1 neck is repeatable and is more mechanically compliant than the HybridIII ATD neck model, but offers significantly greater reaction kinetics relative to necks from post mortem subjects. In contrast, head kinematics, particularly angular acceleration, matched to within 30% of the literature values selected in our limited study. The phase 1 neck proved robust and experienced approximately 100 impacts without mechanical failure. Our ongoing work will continue to refine the neck against data from post mortem subjects while also attempting to validate against data from athletes subjected to head impact.

## ACKNOWLEDGEMENTS

The authors wish to acknowledge Chris Withnall of Biokinetics and Associates (Canada) for his input and consultations on identifying design goals. This work was financially supported by the Natural Sciences and Engineering Research Council (Canada) through Engage Grants (2016) and Discovery Grants (2016 through 2017). Equipment used in this work was purchased with financial support from the Canada Foundation for Innovation – Leader Opportunity Fund; The Pashby Sport Safety Fund; and the Faculty of Engineering at the University of Alberta.

## REFERENCES

ADVANI, S.H., POWELL, W.R., HUSTON, J., OJALA, S.H. (n.d.). Human Head Impact Response: Experimental Data and Analytical Simulations. West Virginia University, Morgantown, WV, 26506.

- ASTM (2016). Standard Performance Specification for Ice Hockey Helmets DOI: 10.1520/F1045-16. ASTM International, West Conshohocken, PA.
- BILLETTE, J., JANZ, T. (2015). Injuries in Canada: Insights from the Canadian Community Health Survey. Retrieved September 2016, from <https://www.statcan.gc.ca/pub/82-624-x/2011001/article/11506-eng.htm>
- CAMACHO, D.L., NIGHTINGALE, R.W., ROBINETTE, J.J., VANGURI, S.K., COATES, D.J., MYERS, B.S. (1997). Experimental Flexibility Measurements for the Development of a Computational Head-Neck Model Validated for Near-Vertex Head Impact (SAE Technical Paper No. 973345).
- CRAWFORD, N.R., PELES, J.D., DICKMAN, C.A. (1998). The Spinal Lax Zone and Neutral Zone: Measurement Techniques and Parameter Comparisons. J Spinal Discord., Vol. 11(5), pp. 416-429.
- KAY, T., ET AL. (1993). Definition of Mild Traumatic Brain Injury. J Head Trauma Rehabil, Vol. 8(3), pp. 86-87. New York, NY: Aspen Publishers Inc.
- KNOWLES, B.M., DENNISON, C.R. (2017). Predicting Cumulative and Maximum Brain Strain Measures from HybridIII Head Kinematics: A Combined Laboratory Study and Post-Hoc Regression Analysis. Annals of Biomedical Engineering, Vol. 45(9), pp. 2146-2158.
- MERTZ, H.J., IRWIN, A.L. (2015). Accidental Injury: Biomechanics and Prevention. New York, NY: Springer Science+Business Media.
- NIGHTINGALE, R.W., CHANCEY, V.C., OTTAVIANO, D., LUCK, J.F., TRAN, L., PRANGE, M., MYERS, B.S. (2006). Flexion and Extension Structural Properties and Strengths for Male Cervical Spine Segments. J Biomech, Vol. 40, pp. 535-542.
- NIGHTINGALE, R.W., WINKELSTEIN, B.A., KNAUB, K.E., RICHARDSON, W.J., LUCK, J.F., MYERS, B.S. (2002). Comparative Strengths and Structural Properties of the Upper and Lower Cervical Spine in Flexion and Extension. J Biomech, Vol. 35, pp. 725-732.
- NOCSAE (2016). Standard Pneumatic Ram Test Method and Equipment Used in Evaluating the Performance Characteristics of Protective Headgear and Face Guards (ND 081).
- PADGAONKAR, A.J., KRIEGER, K.W., KING, A.I. (1975). Measurement of Angular Acceleration of a Rigid Body Using Linear Accelerometers. Journal of Applied Mechanics, Vol. 42(3), pp. 552-556.
- PARACHUTE (2015). The Cost of Injury in Canada. Toronto, ON: Parachute.

- RIZZETTI, A., KALLIERIS, D., SCHIEMANN, P., MATTERN, R. (1997). Response and Injury Severity of the Head-Neck Unit During a Low Velocity Head Impact, IRCOBI Conference, Hannover, September 1997.
- ROWSON, B., ROWSON, S., DUMA, S. M., (2015). Hockey STAR: A Methodology for Assessing the Biomechanical Performance of Hockey Helmets. *Annals of Biomedical Engineering*, Vol. 43(10), pp. 2429-2443. DOI: 10.1007/s10439-015-1278-7.
- SAE International (2003). Surface Vehicle Recommended Practice (J211-1). Retrieved from SAE Standards Online.
- SPARKS, J.L., VAVALLE, N.A., KASTING, K.E., LONG, B., TANAKA, M.L., SANGER, P.A., SCHNELL, K., CONNER-KERR, T.A. (2015). Use of Silicone Materials to Simulate Tissue Biomechanics as Related to Deep Tissue Injury. *Advances in Skin & Wound Care Journal*, Vol. 28, pp. 59-68.
- TAKHOUNTS, E.G., CRAIG, M.J., MOORHOUSE, M., MCFADDEN, J. (2013). Development of Brain Injury Criteria (BrIC). *Stapp Car Crash Journal*, Vol. 57, pp. 243-266.
- UNECE (2002). Uniform Provisions Concerning the Approval of Protective Helmets and Their Visors for Drivers and Passengers of Motor Vehicles and Mopeds (E/ECE/324: E/ECE/Trans/505). Rev.1, Add. 21, Rev.4.
- VASAVADA, A.N., DANARAJ, J., SIEGMUND, G.P. (2008). Head and Neck Anthropometry, Vertebral Geometry and Neck Strength in Height-Matched Men and Women. *J Biomech*, Vol. 41, pp 114-121.
- WHEELDON, J.A., PINTAR, F.A., KNOWLES, S., YOGANANDAN, N. (2004). Experimental Flexion/Extension Data Corridors for Validation of Finite Element Models of the Young, Normal Cervical Spine. *J of Biomech*, Vol. 39, pp. 375-380.
- YOGANANDAN, N., HUMM, J., PINTAR, F.A., WOLFLA, C.E., MAINMAN, D.J. (2011). Lateral Neck Injury Assessments in Side Impact Using Post Mortem Human Subject Tests. In *Proc. AAAM Annual Conference*, Vol. 55, pp. 169-179.